

Supersonic Nozzle Design for Laser-Assisted Oxygen Hybrid Cutting

Gwang Ho Jeong*, Seok Kim**, Young Tae Cho**,#

*Smart Manufacturing Engineering, Changwon National University, **Department of Mechanical Engineering, Changwon National University

레이저 산소 하이브리드 커팅을 위한 초음속 노즐 설계에 관한 연구

정광호*, 김석**, 조영태**

*창원대학교 스마트제조융합협동과정, **창원대학교 기계공학부

(Received 10 May 2021; received in revised form 22 May 2021; accepted 07 June 2021)

ABSTRACT

LASOX is a cutting technology used to dismantle nuclear power plants. The core component of the laser-assisted oxygen hybrid cutting process is the supersonic nozzle. To design optimized supersonic nozzles, an experimental design was established and computational fluid dynamics was used to analyze the supersonic nozzles. The main factors affecting the supersonic nozzle performance were identified using Minitab. Further, the correlations and interactions between the main factors of the supersonic nozzle design were analyzed. The fluid analysis results were examined for the major factors and standardized response variables as well as main effects to ensure suitability of the supersonic nozzle design for the laser-assisted oxygen cutting process.

Key Words : Supersonic Nozzle(초음속 노즐), Laser-assisted Oxygen Cutting(레이저 산소 절단), CFD(전산유체역학), DOE(실험 계획법)

1. Introduction

Nuclear decommissioning is emerging as a crucial technique due to the increasing number of permanently closed and outdated nuclear power plants. However, among the related techniques for proper nuclear decommissioning, a suitable cutting technology must be developed^[1,2]. One method is oxygen cutting, which enables the cutting of thick

materials but produces an significant amount of secondary radioactive waste^[3]. Alternatively, laser cutting involves a smaller amount of kerf and produces less by-products; however, a high-powered laser is required to cut thick materials, and there is a limit to the thickness of material that can be cut. To overcome these drawbacks, a hybrid of oxygen and laser cutting technology can be applied to the dismantling of radioactive metal structures, such as nuclear power plants and steam generators.

The laser-assisted oxygen cutting (LASOX) process, which was first introduced approximately 20

Corresponding Author : ytcho@changwon.ac.kr

Tel: +82-55-213-3600, Fax: +82-55-275-0101

Copyright © The Korean Society of Manufacturing Process Engineers. This is an Open-Access article distributed under the terms of the Creative Commons Attribution-Noncommercial 3.0 License (CC BY-NC 3.0 <http://creativecommons.org/licenses/by-nc/3.0>) which permits unrestricted non-commercial use, distribution, and reproduction in any medium, provided the original work is properly cited.

years ago, utilizes a laser to supplement oxygen cutting to reduce kerf and increase cutting speed. The advent of this technique shortened the preheating time and enabled the cutting of thick sheets, even with a low-power laser, while minimizing thermal impact^[4].

LASOX maximizes the utilization of combustion heat generated from the Fe - O reaction when heating steel to a high temperature using a high-power laser. The cutting nozzle used for LASOX includes a short focal length lens for laser focusing and acts as a gas chamber for supplying oxygen coaxially. Figure 1 shows a schematic diagram of the LASOX process. The focus of the laser beam is placed in the lens housing, and the gas from the nozzle moves directly towards the surface of the base material. The width of the gas jet should be smaller than the diameter of the nozzle at the base material surface to allow the gas jet to be contained within the laser beam diameter, thus enabling every oxygen molecule that touches the surface to undergo a reaction process. More specifically, the nozzle should be designed such that the temperature of the steel surface is heated to over 1000 °C using a laser beam and a gas jet. This paper describes the design process of a supersonic nozzle through a simulation for increasing the efficiency of the LASOX process. Numerical and empirical analyses of the application of supplementary gas in conventional laser cutting techniques are referenced^[5,6]. A flow simulation identified the interactions between the key factors affecting the performance of the supersonic nozzle and supported the suitable design of a LASOX technique.

2. Main Factors of Supersonic Nozzle Design

The structure of supersonic nozzles is an important parameter affecting laser fusion cutting

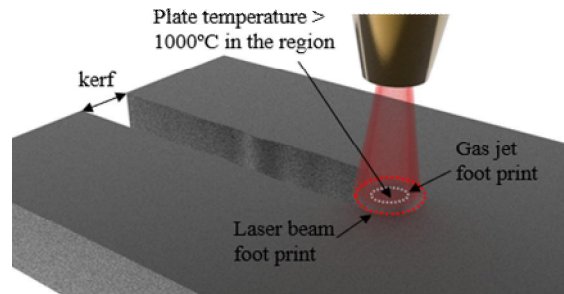


Fig. 1 Schematics of LASOX process

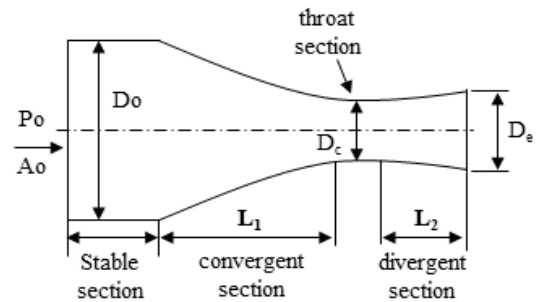


Fig. 2 Schematic Supersonic nozzle

performance because it directly affects the gas flow characteristics. The supersonic nozzle shape generally follows the de-Laval shape, as shown in Figure 2^[7]. To reach $Ma = 1$ (sonic) in the throat, which is a relatively important section in the supersonic nozzle structure, the diameter of the supersonic nozzle inlet must be much larger than the throat diameter, and the converging section should have a larger diameter than the nozzle inlet, as described by equations (1) and (3)^[8-10]. In the converging section, the gas flow is accelerated while maintaining uniform and parallel flow. The factor affecting the characteristics of this section is the convergence ratio (inlet area/throat area), given by equation (2). In the diverging section, the gas flow accelerates even further, and the Mach number at the exit is determined by the area ratio of the nozzle (exit area/throat area), as per equation (4). Therefore, the nozzle area ratio is one of the major

factors in the design of a supersonic nozzle.

$$D_o > \sqrt{5} D_c \quad (1)$$

$$\frac{A_o}{A_c} = \frac{M_c}{M_o} \left(\frac{1 + \frac{\gamma-1}{2} M_o^2}{1 + \frac{\gamma-1}{2} M_c^2} \right)^{\frac{\gamma+1}{2(\gamma-1)}} \quad (2)$$

$A_o =$ Inlet Area (mm^2), $A_c =$ Throat Area (mm^2)
 $M_o =$ Inlet Mach number, $M_c =$ Throat Mach number

$$L_1 \geq D_o \quad (3)$$

$$\frac{A_e}{A_c} = \frac{M_c}{M_e} \left(\frac{1 + \frac{\gamma-1}{2} M_e^2}{1 + \frac{\gamma-1}{2} M_c^2} \right)^{\frac{\gamma+1}{2(\gamma-1)}} \quad (4)$$

$A_e =$ Exit Area (mm^2), $M_e =$ Exit Mach number
 $\gamma =$ specific heat ratio (C_p/C_v)

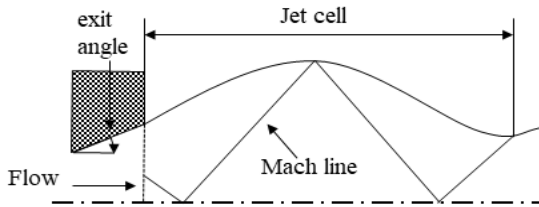


Fig. 3 Exit angle > 0

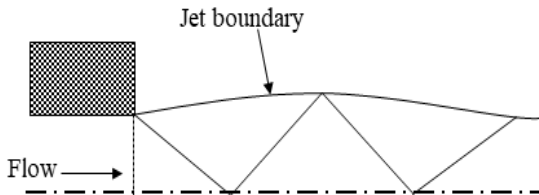


Fig. 4 Exit angle = 0

Figures 3 and 4 display the jet flow diverging from the nozzle exit. As the exit angle of the

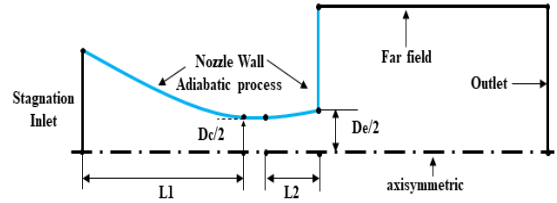


Fig. 5 Computational domain and boundary condition

supersonic nozzle increases, the length of the jet cell shortens because the starting point of the Mach line becomes closer to the centerline of the jet^[11]. According to the study by Chi Zhang and Peng Wen^[12], the jet length of the nozzle flow varies under different stagnation pressure conditions in the supersonic nozzle, and the nozzle pressure ratio (NPR = stagnation pressure/surrounding pressure = P_o/P_b) is an important parameter.

3. Numerical Analysis

3.1 Boundary Conditions and Governing Equations

The ANSYS Fluent commercial computational fluid dynamics package and Reynolds-averaged Navier-Stokes code were employed for the numerical analysis.

Conservation of the mass:

$$\frac{d\rho}{\rho} + \frac{dV}{V} + \frac{dA}{A} = 0, \quad m = \rho VA = \text{constant} \quad (6)$$

$\rho =$ density (kg/m^3), $V =$ velocity (m/s), $A =$ Area (m^2)

Conservation of the momentum:

$$\left(u + \frac{p}{\rho} \right) = \frac{1}{2} V^2 = \text{constant} \quad (7)$$

$u =$ velocity magnitude (m/s), $p =$ pressure (N/m^2 (Pa))

Conservation of the energy:

$$h + \frac{1}{2} V^2 = \text{constant}, \quad h = \text{enthalpy (kJ/kg)} \quad (8)$$

$$\text{ideal gas equation: } P = \rho RT \quad (9)$$

Equations (6) to (9)^[13-15] were the governing equations, applied as density-based and steady-state, assuming isentropic flow and ideal gas. Sutherland's viscosity law was adopted for the viscosity equations. The turbulence model was based on Menter's shear stress transport model^[16], with the inlet as the entry boundary conditions at a temperature of 300 K. A nozzle wall was assumed to be no-slip with insulated boundary conditions. The far-field was set as the boundary of the flow region and with the same conditions as the nozzle wall. The outlet was set to a temperature of 300 K with atmospheric pressure. The flow field area of the outside of the supersonic nozzle was designed to be 500 mm, and axial symmetry was assumed to be at the centerline of the jet in a 2D space.

3.2 Experimental Design

By referring to the supersonic nozzle flow analysis study by Mohammed Darwish^[17], the design of the supersonic nozzle was performed with the CATIA software. The flow analysis was performed by first establishing an experimental design to derive the correlation between the major parameters of a supersonic nozzle and then establishing a 3×2 (factor × level) full fractional design. For the experimental design, the purpose of the experiment had to be determined first. The objective of the supersonic nozzle flow analysis was to compile fundamental experimental cutting data for the decommissioning of nuclear power plants. Because a supersonic nozzle with a constant flow field and maximum jet length must be used to section off nuclear reactors with thick materials during decommissioning, effective jet length [17], Mach number stability, and pressure stability were selected as the response variables. The effective jet length was defined as from the nozzle exit to where the Mach number decreases rapidly, rather than the

length of the supersonic region, as shown in Figure 6. The effective jet length was a measure of performance of the cutting technique for nuclear decommissioning because the length of the jet spray outside of the nozzle exit remains important when cutting. Mach number stability and pressure stability were selected as response variables to implement a constant flow field outside the nozzle exit. This was because flow stability is important for the jet flow outside the supersonic nozzle exit to have the longest and most effective jet length possible. Other major factors of supersonic nozzle design are nozzle area ratio, exit angle, and NPR. The full fractional 3×2 experimental design produced 8 models. The flow analysis was repeated twice, and therefore a total of 16 flow analyses were conducted.

Table 1 Factor & Level

Factor	Low Level	High Level
NPR	5	10
Nozzle Area ratio	1.7	2.68
Exit angle	9°	15°

Table 2 Models 1-8

Nozzle length 15.5mm	Nozzle Area ratio	Exit angle (°)	NPR
model 1	1.7	9	5
model 2	1.7	9	10
model 3	1.7	15	5
model 4	1.7	15	10
model 5	2.68	9	5
model 6	2.68	9	10
model 7	2.68	15	5
model 8	2.68	15	10

The results from the flow analysis had a sufficient degree of freedom in the error. The results were then standardized, and the interactions between key factors or the extent to which factors affected the performance of the nozzle were examined through analysis of variance.

To obtain the Mach number stability in Figure 7, all Mach data inside and outside the nozzle were set as the population of interest, while the region outside of the nozzle exit was sampled. Then, the change deviations were extracted and averaged for the region from the nozzle exit point to the effective jet length. Using the deviation data, the standard deviation was derived for the outside of the nozzle exit. Pressure stability in Figure 8 was derived in the same manner as for obtaining Mach number stability.

$$\text{Mach number stability(\%)} \ \& \ \text{Pressure stability(\%)}: \left(\frac{\text{Standard deviation of nozzle exit}(s)}{\text{Average of deviation}} \right) \times 100 \quad (10)$$

4. Analysis Results and Considerations

4.1 Factor Analysis Results

According to the Mach number results in Figure 9, pressure stability generally decreased in the models with large pressure ratios. Particularly for Model 5, it was seen that the Mach number momentarily dropped to 0.5 as a strong normal shockwave was generated at the exit, and the supersonic flow jet length outside the exit was the shortest.

Model 2 exhibited the highest jet length and most stable data values in terms of pressure stability and Mach number stability. The results were standardized and analyzed using the Minitab software, which produced a Pareto chart standardizing the data by the reaction parameters.

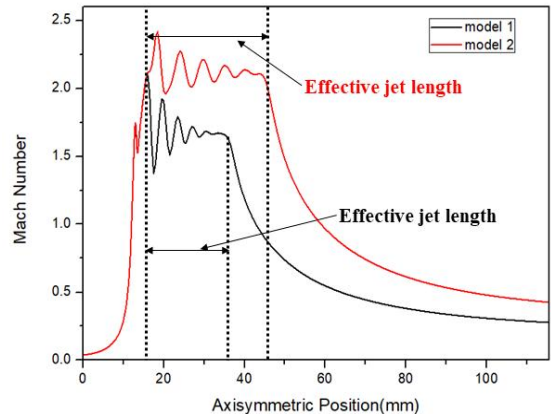


Fig. 6 Effective jet length

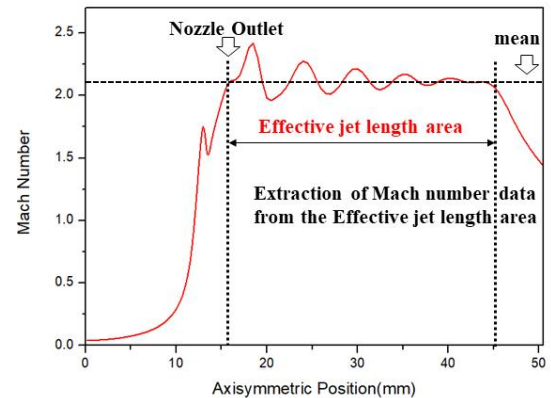


Fig. 7 Mach number stability

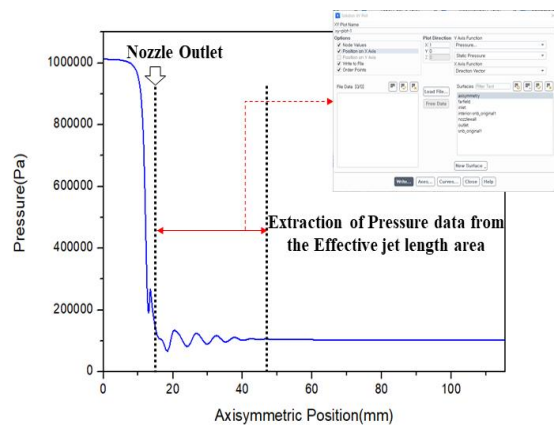


Fig. 8 Pressure stability

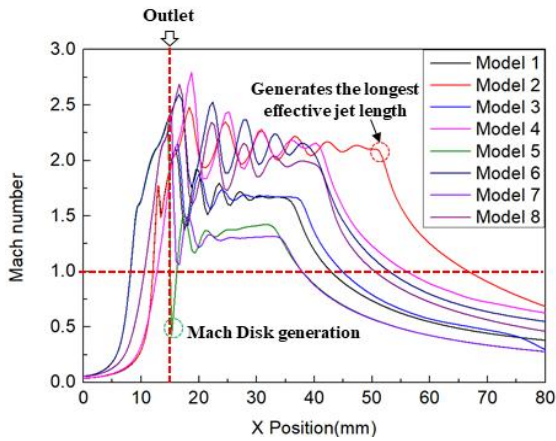


Fig. 9 Result of Mach number graph

In this chart, it can be observed how much each major factor affected the flow outside the supersonic nozzle exit. In the Pareto chart of the effective jet length, NPR had the greatest influence, followed by nozzle area ratio and interaction between the area ratio and exit angle. In the Pareto chart of the Mach number stability (Figure 10), the nozzle area ratio had the largest impact, followed by NPR. Other factors and their interactions, especially the exit angle, did not contribute to the Mach number stability. In the Pareto chart of pressure stability shown in Figure 11, it was found that the nozzle area ratio had the greatest impact, followed by the relationships between the nozzle area ratio and NPR and between the exit angle and NPR.

4.2 Main Effects of Response Variables

Among the main effects on the effective jet length, exit expansion angle had a minimal impact. When increasing the nozzle area ratio, the exit design Mach number increased, resulting in a decrease in effective jet length. Considering the main effects of the Mach number stability, when the nozzle area ratio was high, the Mach number stability increased and the flow outside the nozzle exit became unstable due to relatively large changes

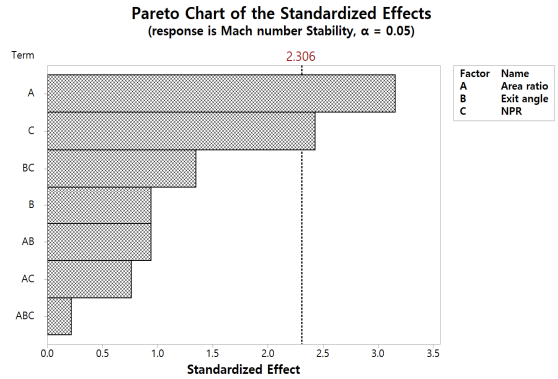


Fig. 10 Pareto Chart of Mach number stability

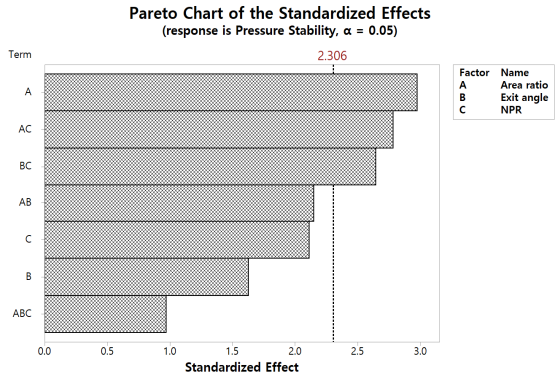


Fig. 11 Pareto Chart of Pressure stability

compared to other factors. When the standard deviation of the Mach number data outside the nozzle exit was large, the Mach number stability generally increased and had a high change rate, thus causing an unstable flow.

$$\left(\frac{\text{Standard deviation of nozzle exit}(s)}{\text{Average of deviation}} \right) \times 100$$

The changes of the exit angle led to improved Mach number stability and unstable flow but showed the smallest change rate compared to other factors. In contrast, when NPR was set at a high level, the reaction factor Mach stability became lower, which led to a reduced change in Mach number outside the nozzle exit, thus forming a

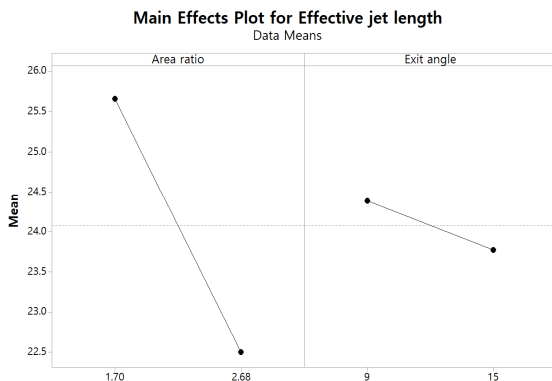


Fig. 12 Main Effects plot for Effective jet length

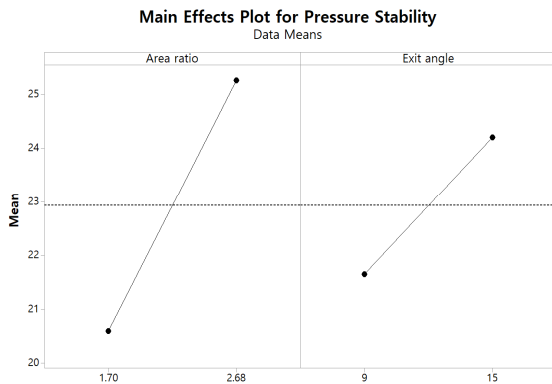


Fig. 13 Main Effects plot for Pressure stability

uniform flow field and improving Mach number stability. When the level of the nozzle area ratio increased, the change rate of the pressure stability was the largest, and the flow became unstable as a result. Furthermore, increasing the nozzle exit angle caused higher pressure stability and unstable flow, while increasing the NPR caused more pressure variation in flow and unstable flow. Thus, it can be inferred that all factors have an impact on pressure variation.

5. Conclusion

Based on the results of supersonic nozzle flow analysis, interactions between major parameters and

significant factors were confirmed through standardization of the results. Ultimately, a higher NPR should be employed when designing a supersonic nozzle, considering effective jet length, Mach number stability, and pressure stability. The nozzle area ratio should be designed at a lower level based on the jet length, Mach number stability, and pressure stability. Lastly, pressure stability decreases as the major factors of nozzle area ratio and exit angle increase, indicating that the nozzle area ratio and exit angle should be lowered during the design process.

Acknowledgement

This study was funded by the National Research Foundation of Korea (NRF-2019R1A5A8083201) (Ministry of Science and ICT) and Regional Intelligence Innovation Talent Training Grant by Institute of Information & Communications Technology Planning and Evaluation (Grand ICT Research Center IITP-2021-2016-0-00318).

REFERENCES

1. Shin, J. S., Oh, S. Y., Park, H., Chung, C. M., Seon, S., Kim, T. S., Lee, L., Lee, J. "Laser cutting of steel plates up to 100mm in thickness with a 6-kW fiber laser for application to dismantling of nuclear facilities." *Optics and Lasers in Engineering*, Vol. 100, pp. 98-104, 2018.
2. Oh, S. Y., Shin, J. S., Kim, T. S., Park, H., Lee, L., Chung, C. M., & Lee, J. "Effect of nozzle types on the laser cutting performance for 60-mm-thick stainless steel." *Optics & Laser Technology*, Vol. 119, pp. 1-9, 2019.
3. Bonavigo, L., De Salve, M., Zucchetti, M., & Annunziata, D. "Radioactivity release and dust production during the cutting of the primary circuit of a nuclear power plant: The case of E.

- Fermi NPP." *Progress in Nuclear Energy*, Vol. 52, No. 4, pp. 359-366, 2010.
4. O'Neill, W., Gabzdyl, J. T., "New developments in laser-assisted oxygen cutting", *Optics and Lasers in Engineering* Vol. 34, No. 4-6, pp. 355-367, 2000.
 5. Yoon, S. K., Sung, H. G., & Lee, Y., "Computational Study of Impingement Characteristics of Assist Gas from Coaxial/Off-axis Nozzles in Laser Machining." *Journal of the Korean Society of Manufacturing Process Engineers*, Vol 9, No. 5, pp. 14-19, 2010.
 6. Son, S. H., Lee, S. J., & Lee, Y., "Experimental Study of Influence of Nozzle Design on Removal of Melted Materials in Laser Cutting Process", *Journal of the Korean Society of Manufacturing Process Engineers*, Vol. 11, No. 1, pp. 33-38, 2012.
 7. Riveiro, A., Quintero, F., Boutinguiza, M., Del Val, J., Comesaña, R., Lusquiños, F., & Pou, J., "Laser cutting: a review on the influence of assist gas", *Materials*, Vol. 12, No. 1, pp. 1-31, 2019.
 8. Darwish, M., Orazi, L., & Angeli, D., "Simulation and analysis of the jet flow patterns from supersonic nozzles of laser cutting using OpenFOAM", *The International Journal of Advanced Manufacturing Technology*, Vol. 102, pp. 3229-3242, 2019.
 9. Man, H. C., Duan, J., & Yue, T. M., "Design and characteristic analysis of supersonic nozzles for high gas pressure laser cutting", *Journal of Materials Processing Technology*, Vol. 63, No. 1-3, pp. 217-222, 1997.
 10. Man, H. C., Duan, J., Yue, T. M., & Dong, P., "Design of supersonic nozzle for laser cutting with high pressure gas", *International Congress on Applications of Lasers & Electro-Optics. Laser Institute of America.*, Vol. 1997, No. 1, pp. B118-B127, 1997.
 11. Kim, H. D., & Sin, H. S., "Numerical Study on Under-Expanded Jets through a Supersonic Nozzle (II).", *Transactions of the Korean Society of Mechanical Engineers B*, Vol. 20, No. 6, pp. 1994-2004, 1996.
 12. Zhang, C., Wen, P., Yuan, Y., & Fan, X., "Evaluation and optimal design of supersonic nozzle for laser-assisted oxygen cutting of thick steel sections." *The International Journal of Advanced Manufacturing Technology*, Vol. 86, No. 5, pp. 1243-1251, 2016.
 13. Ramesh Kumar, R., & Devarajan, Y., "CFD simulation analysis of two-dimensional convergent-divergent nozzle", *International Journal of Ambient Energy*, Vol. 41, No. 13, pp. 1505-1515, 2020.
 14. Shariatzadeh, O. J., Abrishamkar, A., & Jafari, A. J., "Computational Modeling of a Typical Supersonic Converging-Diverging Nozzle and Validation by Real Measured Data", *Journal of Clean Energy Technologies*, Vol. 3, No. 3, pp. 220-225, 2015.
 15. Jagtap, R., "Theoretical & CFD Analysis Of De Laval Nozzle", *International Journal of Mechanical and Production Engineering*, Vol. 2, pp. 33-36, 2014.
 16. Kam, H. D., & Kim, J. S., "Assessment and validation of turbulence models for the optimal computation of supersonic nozzle flow", *Journal of the Korean Society of Propulsion Engineers*, Vol. 17, No. 1, pp. 18-25, 2013.
 17. Darwish, M., Mrña, L., Orazi, L., & Reggiani, B., "Modeling and analysis of the visualized gas-assisted laser cutting flow from both conical and supersonic nozzles", *The International Journal of Advanced Manufacturing Technology*, Vol. 106, No. 9, pp. 4635-4644, 2020.